9.50; S, 15.07. Found: C, 67.85; H, 9.74; S, 14.81.

Method B: Claisen condensation reaction of methyl ketones with thionoesters using sodium amide as base as described previously for the preparation of aromatic β-thioxo ketones (R^1 and/or R^3 = aryl, R^2 = H),[9] **2-thioacetylcyclohexanone (23)**,[20] and **1-(1-methylcyclopropyl)-3-thioxobutan-1-one (8)**.[44] The method applies apparently generally to 2-thioacylcycloalkanones and, with limitations, to open-chain β-thioxo ketones.[1]

2-Methyl-6-thioxoheptan-4-one (2): yellow oil; bp 42 °C (0.15 mmHg); yield 77%. Anal. Calcd for $C_8H_{14}OS$: C, 60.74; H, 8.92; S, 20.23. Found: C, 60.64; H, 9.05; S, 19.62.

1-Cyclopropyl-3-thioxobutan-1-one (4): yellow oil; bp 103-104 °C (13 mmHg); yield 63%. Anal. Calcd for $C_7H_{10}OS$: C, 59.12; H, 7.09; S, 22.95. Found: C, 59.06; H, 6.95; S, 22.52.

2-Methyl-5-thioxohexan-3-one (5): yellow oil; bp 75-76 °C (10 mmHg); yield 41%. Anal. Calcd for $C_7H_{12}OS$: C, 58.31; H, 8.39; S, 22.20. Found: C, 58.55; H, 8.51; S, 22.02.

4-Thioxohexan-2-one (11): yellow oil; bp 67-68 °C (9 mmHg); yield 52%. Anal. Calcd for $C_6H_{10}OS$: C, 55.37; H, 7.75; S, 24.59. Found: C, 55.31; H, 7.85; S, 24.60.

2-Methyl-6-thioxooctan-4-one (13): yellow oil; bp 65-66 °C (0.2 mmHg); yield 67%. Anal. Calcd for $C_9H_{16}OS$: C, 62.76; H, 9.36; S, 18.58. Found: C, 63.22; H, 9.62; S, 18.55.

1-Cyclopropyl-3-thioxopentan-1-one (15): yellow oil; bp 58 °C (0.14 mmHg); yield 34%. Anal. Calcd for $C_8H_{12}OS$: C, 61.52; H, 7.75; S, 20.49. Found: C, 61.61; H, 7.80; S, 19.95.

2-Methyl-5-thioxoheptan-3-one (16): yellow oil; bp 53-55 °C (0.25 mmHg); yield 37%. Anal. Calcd for $C_8H_{14}OS$: C, 60.74; H, 8.92; S, 20.23. Found: C, 60.74; H, 9.03; S, 19.65.

2-Thioacetyl-4-methylcyclohexanone (24): yellow oil; bp 98-99 °C (0.35 mmHg); yield 45%. Anal. Calcd for $C_9H_{14}OS$: C, 63.51; H, 8.29; S, 18.80. Found: C, 63.42; H, 8.52; S, 18.81.

2-Thioacetyl-4-*tert*-butylcyclohexanone (25): light yellow crystals; mp 58-59 °C (hexane); yield 44%. Anal. Calcd for $C_{12}H_{20}OS$: C, 67.89; H, 9.50; S, 15.07. Found: C, 68.08; H, 9.55; S, 14.90.

2-Thiopropionylcyclohexanone (26): yellow oil; bp 85 °C (0.2 mmHg); yield 63%. Anal. Calcd for $C_9H_{14}OS$: C, 63.51; H, 8.29; S, 18.80. Found: C, 63.61; H, 8.31; S, 18.22.

2-Thiopropionyl-4-methylcyclohexanone (27): yellow oil; bp 97 °C (0.3 mmHg); yield 48%. Anal. Calcd for $C_{10}H_{16}OS$: C, 65.19; H, 8.75; S, 17.36. Found: C, 65.42; H, 8.78; S, 17.17.

2-Thiopropionyl-4-*tert*-butylcyclohexanone (28): yellow oil; bp 138 °C (0.4 mmHg); yield 47%. Anal. Calcd for $C_{13}H_{22}OS$: C, 68.99; H, 9.80; S, 14.14. Found: C, 68.86; H, 9.98; S, 14.00.

Method C: Claisen condensation reaction of methyl ketones with thionoesters with *t*-BuLi as base, as described in the preliminary paper.[1] This method was developed as a direct consequence of the synthetic requirements set up by the intentions of this work. As demonstrated[1] by the successful syntheses of **2,2-dimethyl-6-thioxoheptan-4-one (3)**, **5-methyl-2-thioxoheptan-4-one (6)**, **1-cyclohexyl-3-thioxobutan-1-one (7)**, **2,2-dimethyl-5-thioxohexan-3-one (9)**, **1-(1-adamantyl)-3-thioxobutan-1-one (10)**, **2,2-dimethyl-6-thioxooctan-4-one (14)**, **3-methyl-6-thioxooctan-4-one (17)**, **1-cyclohexyl-3-thioxopentan-1-one (18)**, **1-(1-methylcyclopropyl)-3-thioxopentan-1-one (19)**, **2,2-dimethyl-5-thioxoheptan-3-one (20)**, and **1-(1-adamantyl)-3-thioxopentan-1-one (21)**, this method is superior to method B not only with respect to broadness of applicability but also as regards yields. **3-Methyl-2-thioxohexan-4-one (32)** was obtained in good yield by method B as well as by method C.[1]

Acknowledgment. About 600 UV spectra were recorded to ensure consistency of the reported data. We are grateful to Pia Bjerregaard, Tove Buhl, and Lonny Hallberg for carrying out this task. Thanks are due to Marianne Wehmeyer and Kirsten Bistrup and to the Department of General and Organic Chemistry, The H. C. Ørsted Institute, University of Copenhagen, for the recordings of the 90-MHz ^1H NMR spectra. The Varian HA 100 spectrometer used for the measurements of the ^1H NMR spectra of β-thioxo ketones in CCl_4 solution was kindly placed at our disposal by the Department of Chemical Physics of The H. C. Ørsted Institute. We are grateful to Jonas Pedersen and Else Dayan for helpful instruction and cooperation for these measurements. The microanalyses were kindly performed by Preben Hansen of the Microanalytical Laboratory of The H. C. Ørsted Institute. Finally, we express our gratitude to Allen Sawitz and Claus Danø Møller for guidance by the computations, to Ingrid Jensen for the drawings, to professor Eigil Praestgaard for helpful discussions, and to Tove, Charlotte, and Anja for forbearance.

Registry No. 1, 14660-20-9; **2**, 99618-89-0; **3**, 99618-90-3; **4**, 99618-91-4; **5**, 99618-92-5; **6**, 99618-93-6; **7**, 99618-94-7; **8**, 87505-88-2; **9**, 15591-64-7; **10**, 99618-95-8; **11**, 81674-19-3; **12**, 57711-65-6; **13**, 99618-96-9; **14**, 99618-97-0; **15**, 99618-98-1; **16**, 99618-99-2; **17**, 99619-00-8; **18**, 99619-01-9; **19**, 99619-02-0; **20**, 99619-03-1; **21**, 99619-04-2; **22**, 99619-05-3; **23**, 15578-82-2; **24**, 99619-06-4; **25**, 99619-07-5; **26**, 99619-08-6; **27**, 99619-09-7; **28**, 99619-10-0; **29**, 76698-82-3; **30**, 99619-11-1; **31**, 99619-12-2.

Supplementary Material Available: Tables of complete UV and ^1H NMR spectra data for β-thioxo ketones **1-31** (25 pages). Ordering information is given on any current masthead page.

Dissociative Electron Transfer. Homogeneous and Heterogeneous Reductive Cleavage of the Carbon–Halogen Bond in Simple Aliphatic Halides

Claude P. Andrieux, Iluminada Gallardo,[1] Jean-Michel Savéant,* and Khac-Binh Su

Contribution from the Laboratoire d'Electrochimie de l'Université de Paris 7, Unité associée au CNRS, 75251 Paris, Cedex 05, France. *Received August 9, 1985*

Abstract: The kinetics of the reductive cleavage of the carbon–halogen bond in a series of *n*-, *sec*-, and *tert*-butyl halides are investigated as an example of dissociative electron-transfer processes. The heterogeneous (direct electrochemical reduction at an inert electrode) and homogeneous (electrochemical reduction mediated by aromatic anion radicals) cleavages were found to obey the same activation–driving force free-energy relationship. It is consistent with a concerted electron transfer–bond breaking mechanism, having as the origin of the driving force scale the standard potential of the $RX/R\cdot + X^-$. The activation–driving force relationship is nonlinear and can be approximated by a Hush–Marcus-type quadratic equation. When varying the halogen, from Cl to Br and to I, the reductive cleavage is both thermodynamically easier and kinetically faster at the standard state. The kinetics thus amplifies the thermodynamics in governing reduction potential $RX/R\cdot + X^-$ a given current density. While the essential factor determining the standard potential of the $RX/R\cdot + X^-$ couple is the energy of the carbon halogen bond, the standard activation free energy appears as mainly governed by the ease of the carbon–halogen bond stretching.

The reductive cleavage of the carbon–halogen bond in aliphatic halides (RX) upon addition of one electron is one of the simplest examples of dissociative electron transfer in the organic field. Unlike the case of aromatic halides,[2] there is evidence that a

0002-7863/86/1508-0638$01.50/0

discrete anion radical, $RX^{-}\cdot$, is not an intermediate in the reduction of a simple alkyl halide.[3-6] The reaction thus appears as a concerted electron transfer–bond breaking process.

What are the kinetic characteristics of such reactions in terms of activation vs. driving force free-energy relationships is the main question we want to address in the following analysis of direct and mediated electrochemical reduction of a series of butyl halides. The same problem has been amply investigated, under the form of experimental testing of the Hush–Marcus theory[7] in the case of outer-sphere electron-transfer reactions to an organic molecule, giving rise to an ion radical which remains stable within the time scale of the experiment. Several aspects have been examined in this connection: form of the activation–driving force relationship, i.e., variation of the transfer coefficient with the potential in direct electrochemical reaction,[8] relationship between the heterogeneous and homogeneous kinetic characteristics,[2a,9] and effect of solvent polarization.[9,10] No such investigations have been carried out so far in the case of dissociative electron transfer. In the following, we will emphasize the two first above points.

Although a large amount of work has been devoted to the electrochemical reduction of alkyl halides,[11] precise kinetic data are lacking presumably owing to the extreme reactivity of the intermediate radicals, R·, and carbanions, R^{-}, generated upon electron transfer. Of particular importance for the electrochemical studies is the possible reaction of the intermediate R· radicals with the electrode material within the time scale of the experiment. This is obviously the case with mercury which has often been used as electrode material.[11] Glassy carbon and gold were used in the study reported below. They proved sufficiently inert to give approximately the same kinetic features which showed no critical dependency upon electrode pretreatments. Since the reduction wave of the alkyl chlorides is very close to the discharge of the supporting electrolyte, the investigation was restricted to the bromides and iodides.

The kinetics of the homogeneous electron transfer to alkyl halides was investigated as a function of the driving force of the reaction using a series of aromatic hydrocarbon and heterocycle anion radicals generated at the electrode surface and shuttling electrons to the alkyl halide in the diffusion layer. The variations of the linear sweep voltammetric peak current of these mediators upon addition of the alkyl halides were then used for obtaining the rate constant of the homogeneous electron transfer between each anion radical and each alkyl halides in a series comprising *n*-, *sec*- and *tert*-butyl iodides, bromides, and chlorides.

In the previously investigated case of aryl halides, the application of this redox catalysis method[2,12,13] is straightforward in the sense that there is no significant interaction between the catalyst couple and the species resulting from the aryl halide anion radical. The catalyst further transfers one electron to the aryl radical resulting from the cleavage of the aryl halide anion radical, thus leading to a catalytic overall reaction involving two mediator molecules for the reduction of one molecule of substrate. This is not always the case here since the mediator anion radical competitively transfers one electron to the alkyl radical R· and couples with it leading to reductive alkylation of the mediator:[14]

$$P + e \rightleftarrows Q^{-}\cdot \text{ (standard potential: } E^{\circ}_{PQ}) \qquad (0)$$

$$Q^{-}\cdot + RX \xrightarrow{k_1} R\cdot + X^{-} + P \qquad (1)$$

$$Q^{-}\cdot + R\cdot \xrightarrow{k_2} R^{-} + P \qquad (2)$$

$$Q^{-}\cdot + R\cdot \xrightarrow{k_3} QR^{-} \qquad (3)$$

The ensuing carbanions reacting further with the starting halides or with proton donors present in the reaction medium. Reaction pathway (0) + (1) + (2) then corresponds to a catalytic process with a 2Q per RX stoichiometry as in the case of aryl halides, whereas reaction pathway (0) + (1) + (3) is not catalytic and corresponds to a two-electron per molecule reductive alkylation of the mediator. It has been shown that the addition reaction (3) tends to prevail over the electron-transfer reaction (2) as one passes from the primary to the secondary and to the tertiary alkyl halides for a given mediator and a given halogen.[14c] As will be shown in the following, the same trend is observed, for a given RX, as the standard potential of the mediator redox couple is more and more positive. Also for a given R and a given mediator, the same trend appears when passing from Cl to Br and to I. Cases can thus be found where the addition reaction completely prevails over reaction 2, the process then leading to the formation of an alkylation product along a two electron per mole stoichiometry catalysis being prevented by continuous degradations of the catalyst. It should be noted that the alkylation process may involve another mechanism, that of the electron-transfer radical-coupling mechanism ((1) + (3)) sketched above, viz., an S_N2 nucleophilic displacement mechanism:

$$Q^{-}\cdot + RX \rightarrow QR\cdot + X^{-}$$

(1) Permanent address: Departmento de Quimica-Fisica. Facultad de Ciencias. Universitad Autònoma de Barcelona, Bellaterra (Barcelona), Spain

(2) (a) Andrieux, C. P.; Blocman, C.; Dumas-Bouchiat, J. M.; Savéant, J. M. *J. Am. Chem. Soc.* **1979**, *101*, 3431. (b) Andrieux, C. P.; Blocman, C.; Dumas-Bouchiat, J. M.; M'Halla, F.; Savéant, J. M. *J. Am. Chem. Soc.* **1980**, *102*, 3806.

(3) Low-temperature γ irradiation coupled with ESR characterization of the resulting species[4a] has showed that polarizable dipole (R·)–charge (X^{-}) loose adducts rather than covalently bonded anion radicals are formed upon electron transfer.[4b-f] These are expected to cleave upon raising the temperature.[4e,f] Ab initio quantum chemical calculations gave conflicting results in the case of CH_3Cl + e, one predicting the existence of a discrete anion radical,[5a] the other being in agreement with the formation of a loose complex between CH_3· and Cl^{-}.[5d] Pulse radiolysis investigations also concluded that a discret anion radical does not exist, in the case of simple aliphatic halides.[6]

(4) (a) Symons, M. C. R. *Pure Appl. Chem.* **1981**, *53*, 223. (b) Sprague, E. D.; Williams, F. *J. Chem. Phys.* **1971**, *54*, 5425. (c) Mishra, S. P.; Symons, M. C. R. *J. Chem. Soc., Perkin Trans. 2* **1973**, 391. (d) Symons, M. C. R. *J. Chem. Soc., Chem. Commun.* **1977**, 403. (e) Symons, M. C. R. *J. Chem. Res., Symp.* **1978**, 360. (f) Sprague, E. D. *J. Phys. Chem.* **1979**, *83*, 849.

(5) (a) Canadell, E.; Karofiloglou, P.; Salem, L. *J. Am. Chem. Soc.* **1980**, *102*, 855. (b) Clark, T. *J. Chem. Soc., Chem. Commun.* **1981**, 515. (c) Peyerimhoff, S. D.; Buenker, R. J. *Chem. Phys. Lett.* **1976**, *65*, 434.

(6) (a) Wentworth, W. E.; Becker, R. S.; Tung, R. *J. Phys. Chem.* **1967**, *71*, 1952. (b) Wentworth, W. E.; George, R.; Keith, H. *J. Chem. Phys.* **1969**, *51*, 1791. (c) Kojima, T.; Tanaka, Y.; Satouchi, M. *Anal. Chem.* **1976**, *48*, 1760.

(7) (a) Marcus, R. A. *J. Chem. Phys.* **1956**, *24*, 966. (b) Hush, N. S. *J. Chem. Phys.* **1958**, *28*, 962. (c) Marcus, R. A. *Annu. Rev. Phys. Chem.* **1964**, *15*, 155. (d) Marcus, R. A. *Faraday Discuss. Chem. Soc.* **1982**, *72*, 7.

(8) (a) Savéant, J. M.; Tessier, D. *J. Electroanal. Chem.* **1975**, *65*, 57. (b) Savéant, J. M.; Tessier, D. *J. Phys. Chem.* **1977**, *81*, 2192. (c) Savéant, J. M.; Tessier, D. *J. Phys. Chem.* **1978**, *82*, 1723. (d) Garreau, D.; Savéant, J. M.; Tessier, D. *J. Phys. Chem.* **1979**, *83*, 3003. (e) Savéant, J. M.; Tessier, D. *Faraday Discuss. Chem. Soc.* **1982**, *74*, 57.

(9) Kojima, H.; Bard, A. J. *J. Am. Chem. Soc.* **1975**, *97*, 6317.

(10) (a) Peover, M. E.; Powell, J. S. *J. Electroanal. Chem.* **1969**, *20*, 427. (b) Falsig, M.; Lund, H.; Nadjo, L.; Savéant, J. M. *Nouv. J. Chim.* **1980**, *4*, 445. (c) Fawcet, W. R.; Jawovski, J. S. *J. Phys. Chem.* **1983**, *87*, 2972–6.

(11) (a) Hawley, M. D. In "Encyclopedia of Electrochemistry of the Elements"; Bard, A. J., Lund, H., Eds.; Marcel Dekker: New York, 1980; Vol. XIV, Organic Section. (b) Becker, J. Y. "The Chemistry of Functional Groups, Supplement D", Patai, S., Rappoport, Z., Eds.; Wiley: New York, 1983; Chapter 6, pp 203–285.

(12) (a) Andrieux, C. P.; Dumas-Bouchiat, J. M.; Savéant, J. M. *J. Electroanal. Chem.* **1978**, *87*, 39. (b) *J. Electroanal. Chem.* **1978**, *87*, 55. (c) *J. Electroanal. Chem.* **1978**, *88*, 27. (d) Andrieux, C. P.; Blocman, C.; Savéant, J. M. *J. Electroanal. Chem.* **1979**, *79*, 413. (e) Andrieux, C. P.; Dumas-Bouchiat, J. M.; Savéant, J. M. *J. Electroanal. Chem.* **1970**, *113*, 1. (f) Savéant, J. M.; Su, K. B. *J. Electroanal. Chem.* **1984**, *171*, 341. (h) Andrieux, C. P.; Merz, A.; Savéant, J. M.; Tomahogh, R. *J. Am. Chem. Soc.* **1984**, *106*, 1957.

(13) (a) Evans, D. H.; Naxian, X. *J. Electroanal. Chem.* **1982**, *133*, 367. (b) Griggio, L. *J. Electroanal. Chem.* **1982**, *140*, 315. (c) Evans, D. H.; Naxian, X. *J. Am. Chem. Soc.* **1983**, *105*, 355. (d) Boujlel, K.; Martigny, P.; Simonet, J. *J. Electroanal. Chem.* **1983**, *144*, 437. (e) Rustling, J. P.; Connors, T. F. *Anal. Chem.* **1983**, *55*, 776. (f) Connors, T. F.; Rustling, J. P. *J. Electrochem. Soc.* **1983**, 1120. (g) Capobianco, C.; Farnia, G.; Severin, M. G.; Vianello, E. *J. Electroanal. Chem.* **1984**, *165*, 251. (h) Avaca, L. A.; Gonzalez, E. R.; Titranelli, E. A. *Electrochim. Acta* **1983**, *28*, 1413. (i) Maia, H. L. S.; Madeiros, M. S.; Montenegro, M. I.; Coust, D. D.; Pletcher, D. *J. Electroanal. Chem.* **1984**, *164*, 347.

(14) (a) Bank, S.; Jackett, D. A. *J. Am. Chem. Soc.* **1975**, *97*, 567. (b) *J. Am. Chem. Soc.* **1976**, *98*, 7742. (c) Simonet, J.; Michel, M. A.; Lund, H. *Acta Chem. Scand., Ser. B* **1975**, *B29*, 489.

$$QR\cdot + Q^{-}\cdot \rightarrow QR^{-} + P$$

The latter process does not seem to interfer to a large extent in view of the fact that the yields of reduction and alkylation products do not vary much with the nature of the halogen in the reaction of 5-hexenyl halides with sodium naphthalenide in 1,2 dimethoxyethane.[15a,b] This was confirmed by a stereochemical investigation of the reaction of anthracene anion radicals with optically active 2-octyl halides in ether with Li^+ as the countercation[15c,d] and in DMF with NBu_4^+ as the countercation (i.e., the same reaction medium as used in the study described below):[15d] although the yield of the inverted alkylated product increases slightly when passing from I to Cl, it remains small, less than 11% in all cases.

Previous determinations of the rate constant of the primary electron-transfer reaction (1) are of two kinds. One concerns the reaction of alkyl halides with aromatic anion radicals generated by reaction of the hydrocarbon with an alkali metal in an ethereal solvent.[14a,b,15b,16] The kinetics of the reaction is then strongly influenced by ion pairing between the anion radical and the alkaline countercation.[14a,b]

Another approach was to use the variations of the electrochemical response of the mediator upon addition of the alkyl halide for determining the rate constant.[17] The solvents were Me_2SO and DMF with tetraalkylammonium salts as the supporting electrolyte. Ion pairing is then expected to be insignificant. Unfortunately, the resulting data reported in a recent review[11b] do not appear reliable owing to the fact that appropriate theoretical analyses were not used to extract the rate constant from the electrochemical response. In one case,[17a] the possible catalytic character of the wave was ignored, the linear sweep voltammetric data being treated in the context of a first-order reaction following the electrode electron transfer to the mediator without (even partial) regeneration of the mediator by the follow-up reaction. In the other cases, the polarographic[17b] or potential step chronoamperometric[17c] data were analyzed in the framework of a purely catalytic process, without taking into account the competition with the alkylation reaction. In all cases, the consumption of the substrate was not taken into account.

Extraction of the rate constant k_1 from electrochemical data in the context of the reaction sequence (0)–(3) is not in fact a straightforward problem; all the more that another competing pathway, i.e., the reduction of the R· radical at the electrode surface

$$R\cdot + e \rightleftarrows R^{-} \qquad (2')$$

should in principle be also taken into account. R· is thus the object of a three-cornered competition: reduction at the electrode surface, reduction in the solution by the reduced form of the mediator, and addition on the latter species. The theoretical analysis of this mechanistic problem has been recently carried out.[18] This was used to extract the rate constant k_1 from the linear sweep voltammetric data obtained for the indirect reduction of the nine butyl halides mediated by a series of aromatic hydrocarbon and heterocycle anion radicals.[19,20]

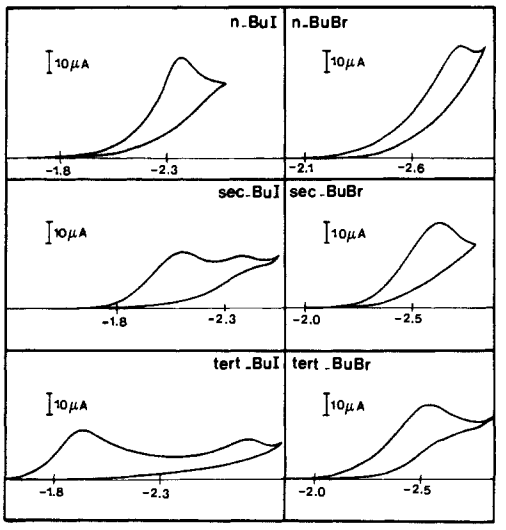

Figure 1. Cyclic voltammetry of primary, secondary, and tertiary butyl iodides and bromides on a glassy carbon electrode in DMF + 0.1 M NBu_4BF_4 at 10 °C. Sweep rate: 0.1 $V\cdot s^{-1}$. C°_{RX} = 2 mM.

Table I. Characteristics of the Electrochemical Reduction of Butyl Iodides and Bromides[a]

compound	no. of waves	peak potential at 0.1 $V\cdot s^{-1}$ (V vs. SCE)	av value[b] of α from peak width at 0.1 $V\cdot s^{-1}$	app no. of electrons at the first wave[c]
n-BuI	1	−2.33	0.30	2.3
n-BuBr	1	−2.85	0.25	2.2
sec-BuI	2	−2.05	0.33	1.2
sec-BuBr	1	−2.63	0.25	2.0
t-BuI	2	−1.91	0.32	1.2
t-BuBr	1	−2.51	0.20	1.9

[a] At glassy carbon, in DMF + 0.1 M NBu_4BF_4, at 10 °C. [b] Assuming the Butler–Volmer kinetics applies.

We will then use the kinetic data thus obtained for both the heterogeneous and homogeneous electron transfer to the various butyl halides to investigate the activation–driving force free-energy relationships characterizing each of these processes and compare them in this respect. This requires the knowledge of the standard potentials of the $RX + e \rightleftarrows R\cdot + X^-$ reaction. Since these data cannot be obtained experimentally, we will have recourse to an estimation based on thermodynamic cycles similar to previously described procedures.[21] A similar analysis has been recently carried out in the case of a highly conjugated benzylic-type chloride, giving rise upon reduction to stable R· radical and R^- carbanion.[22] In this particular case, the value of $E^{\circ}_{RX/R\cdot+X^-}$ could be determined experimentally by using both direct electrochemistry and catalytic data obtained with very positive mediator couples which react with the halide along a predissociation mechanism.[12h] The $R\cdot/R^-$ couple generated from the electrochemical reduction

(15) (a) Garst, J. F.; Barbas, J. T.; Barton, F. E. *J. Am. Chem. Soc.* **1968**, *90*, 7159. (b) Garst, J. F. *Acc. Chem. Res.* **1971**, *4*, 400. (c) Malissard, M.; Mazaleyrat, J. P.; Welvart, Z. *J. Am. Chem. Soc.* **1977**, *99*, 6933. (d) Hebert, E.; Mazaleyrat, J. P.; Welvart, Z.; Nadjo, L.; Savéant, J. M. *Nouv. J. Chim.* **1985**, *9*, 75.

(16) (a) Garst, J. F.; Barton, F. E. *J. Am. Chem. Soc.* **1974**, *96*, 523. (b) Garst, J. F.; Abels, B. N. *J. Am. Chem. Soc.* **1975**, *97*, 4926.

(17) (a) Margel, S.; Levy, M. *J. Electroanal. Chem.* **1974**, *56*, 259. (b) Sease, W. J.; Reed, C. R. *Tetrahedron Lett.* **1975**, 393. (c) Britton, W. E.; Fry, A. J. *Anal. Chem.* **1975**, *47*, 95.

(18) (a) Savéant, J. M.; Su, K. B. *J. Electroanal. Chem.* **1985**, *136*, 1. (b) Nadjo, L.; Savéant, J. M.; Su, K. B. *J. Electroanal. Chem.* **1985**, *196*, 23. (c) Savéant, J. M.; Su, K. B., in preparation.

(19) (a) The data obtained with the three *n*-butyl halides have already been briefly mentioned under the form of log k_1 vs. E°_{PQ} plots in the purpose of comparison with the kinetic data obtained for the reaction of the same halides with a series of iron(I) porphyrins.[19b] (b) Lexa, D.; Mispelter, J.; Savéant, J. M. *J. Am. Chem. Soc.* **1981**, *103*, 6806.

(20) Kinetic data for the reaction of alkyl halides on other electron-rich reagents, mainly low oxidation states of metal complexes, are also available. In most cases, an addition product resulting from the substitution of the halide ion by the metal center ensues. It is not then ascertained that these reactions occur along an electron-transfer mechanism rather than an S_N2 nucleophilic displacement reaction or an atom-transfer reaction. As discussed recently,[22] the two latter reaction pathways have been shown to predominate in several cases. The very rough correlation between the rate constant and the driving force (±3 orders of magnitude dispersion in rate constants) observed with these complexes together with other reducing agents[21b] does not therefore indicate that the same outer-sphere electron-transfer mechanism proceeds in all cases. A more precise analysis of the activation–driving force relationships clearly shows that these are not the same for, e.g., aromatic anion radicals (outer-sphere electron transfer) and iron(I) porphyrins (inner-sphere mechanism): for the same value of the standard potential, the latter are more reactive than the former toward *n*-butyl halides by several orders of magnitude.[19b]

(21) (a) Hush, N. S. *Z. Elektrochem.* **1957**, *61*, 734. (b) Eberson, L. *Acta Chem. Scand., Sect. B* **1982**, *B36*, 533.

(22) Andrieux, C. P.; Merz, A.; Savéant, J. M. *J. Am. Chem. Soc.* **1985**, *107*, 6097.

of the halide is able to redox-catalyze the electrochemical reaction, giving rise to an autocatalytic process. This is the only homogeneous redox catalysis data in this case. On the other hand, the autocatalytic reaction prevented a detailed investigation of the heterogeneous activation-driving force relationship. A much more detailed analysis of both the heterogeneous and homogeneous electron-transfer kinetics was carried out in the present study. Its analysis had, however, to involve the use of estimated, rather than experimentally measured, standard potential data.

Results

Direct Electrochemistry of Butyl Halides. Figure 1 shows typical cyclic voltammograms obtained with the six butyl iodides and bromides on a glassy carbon electrode in DMF. The main characteristics of the direct electrochemical reduction of these compounds as derived from cyclic voltammetry are summarized in Table I. A single wave is observed in all cases with the exception of *sec*- and *t*-BuI where two successive waves are visible on the cyclic voltammograms. The ease of reduction, as featured by the peak potential of this first (or single) wave, falls in the following order: iodides > bromides whatever R; *t*-Bu > *sec*-Bu > *n*-Bu for both iodides and bromides. In all cases the wave is unusually broad, corresponding to an average value of the transfer coefficient α, in the context of Butler–Volmer kinetics,[23] much below 0.5. In this connection, bromides exhibit systematically lower α values than iodides.

The apparent number of electrons per molecule at the first or at the single wave was estimated by comparison of the peak heights for RX and for anthracene under the same conditions (Table I). It then appears that when a single wave is observed, it corresponds to the exchange of two electrons per molecule, while when two waves are observed the first wave involves a one electron per molecule stoichiometry. It is important to note that the number of waves and the wave heights remain the same upon addition of water (up to 0.5 M) or phenol (up to 0.05 M) to the solution. This shows that under our experimental conditions, the amount of proton donors (mainly residual water) initially present in the medium is sufficient to protonate R^- anions that can be formed upon reduction, preventing them to react with RX itself.

It follows that the appearance of a single two-electron wave (*n*-BuBr, *sec*-BuBr, and *n*-BuI) corresponds to a situation where the R· radicals formed upon one-electron reductive cleavage of the C–X bond are reduced at a potential which is positive or at least equal to the potential at which the reductive cleavage occurs. In the case of *sec*-BuI, the R· radical is not reduced at the potential where the reductive cleavage occurs. R· is then reduced at a more negative potential, giving rise to a second wave. In the case of *t*-BuBr, the shape of the peak seems to indicate that an intermediate situation occurs where the reduction of R· is only very slightly negative to that of RX. These observations fall in line with the relative ease of the reduction cleavage as a function of the halogen and of R as indicated previously and also with the expectation that the ease of reduction of the butyl radicals falls in the order n > sec > tert, resulting from electronic effects. The spacing of the two waves is in addition a function of the ensuing fate of R· radicals when not reduced at the electrode at the potential where they are formed. They are then expected to undergo competitive dimerization and H-atom-transfer disproportionation, involving both the same second-order kinetics. These reactions will tend to shift negatively the reduction potential of R· into R^-. Preliminary attempts to simulate the wave system in the framework of such a reaction mechanism gave satisfactory results. This point will be further developed in a forthcoming publication, combining the above results with an investigation of the kinetics of electron transfer to R· radicals from homogeneous mediators, aiming at an estimation of the standard potential of the $R\cdot/R^-$ couple.[24]

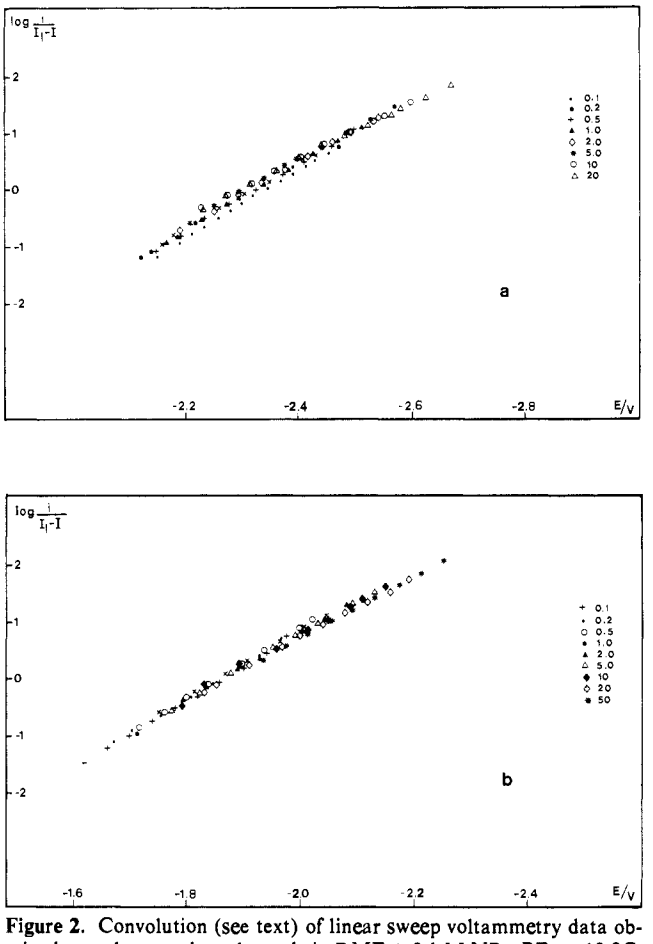

Figure 2. Convolution (see text) of linear sweep voltammetry data obtained at a glassy carbon electrode in DMF + 0.1 M NBu_4BF_4 at 10 °C: (a) *n*-BuI, (b) *t*-BuI.

The results of the convolution analysis[25] of the linear sweep voltammetric data obtained in an extended range of sweep rates are shown in Figure 2. The observed current was convoluted with the time function $(\pi t)^{-1/2}$

$$I = \pi^{-1/2} \int_0^t i(\eta)\ (t-\eta)^{-1/2}\, d\eta$$

and the potential-dependent rate constant of the forward electron transfer at the electrode, $k(E)$, obtained as[8a,25]

$$\log \frac{k(E)}{D^{1/2}} = \log \frac{i}{I_l - I}$$

where I_l is the plateau value of the convoluted current which is reached at potentials beyond the reduction wave and D is the diffusion coefficient. The convolution treatment was carried out for *n*-BuI and *t*-BuI and not for the other iodides and bromides for the following reasons. With *n*-BuBr and *sec*-BuBr, the reduction wave is too close to the discharge of the supporting electrolyte. With *sec*-BuI, the second wave is too close to the first. With *t*-BuBr, the two waves occur approximately at the same potential leading to an increase of the peak width which is not representative of the $RX + e \rightarrow R\cdot + X^-$ reaction. Although there is an important scatter of the data points, the log $[k(E)D^{-1/2}]$ vs.

(23) (a) I.e., ignoring for the moment the possible variation of the transfer coefficient with potential. (b) Delahay, P. "Double Layer and Electrode Kinetics"; Interscience; New York, 1965; Chapter 7. (c) Similar average values of α were obtained in each case from the peak width at a given sweep rate $\alpha = 1.86\ (RT/F)/(E_{p/2} - E_p)$ and from the variations of the peak potential with the sweep rate $\alpha = -(RT/F)/(\partial E_p/\partial \ln v)$.[23d] (d) Matsuda, H.; Ayabe, Y. *Z. Elektrochem.* **1955**, *59*, 494.

(24) (a) Previous work[24b] indicated that R· radicals are more difficult to reduce than the parent RX compounds in several cases. Further investigations have shown this to be erroneous for allylic and benzylic derivatives.[24c,22] It appears that the reduction of R· is effectively more difficult than that of RX for tertiary and secondary alkyl iodides. What remains surprising is that the reversibility of the $R\cdot/R^-$ couple could be reached by using second harmonic AC polarography.[24b] The reactions of R^- with acidic impurities and/or with the starting alkyl halides are indeed expected to be quite fast. (b) Breslow, R.; Grant, J. L., *J. Am. Chem. Soc.* **1977**, *99*, 7745. (c) Bard, A. J.; Merz, A. *J. Am. Chem. Soc.* **1979**, *101*, 2959.

(25) Imbeaux, J. C.; Savéant, J. M. *J. Electroanal. Chem.* **1973**, *44*, 169.

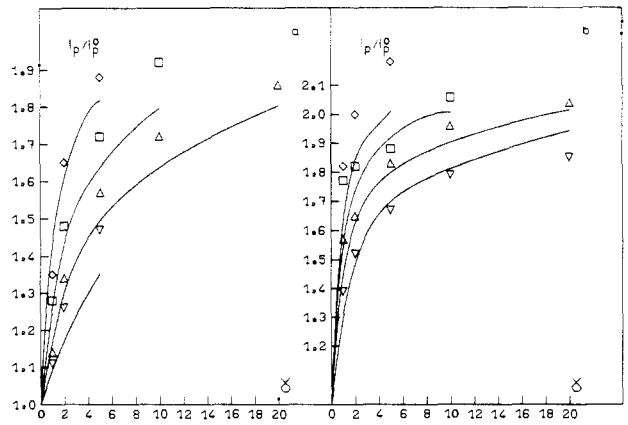

Figure 3. Mediated reduction of *t*-BuBr by methyl benzoate in DMF + 0.1 M NBu_4BF_4 at 10 °C. Variations of the normalized peak current, i_p/i_p°, with the excess factor, $\gamma = C_{RX}^\circ/C_P^\circ$: (a) mediator concentration, C_P° = 1 mM, sweep rate (in $V \cdot s^{-1}$) 2 (◇), 5 (□), 10 (△), 20 (▽); (b) mediator concentration, C_P° = 4 mM, sweep rate (in $V \cdot s^{-1}$) 2 (◇), 5 (□), 10 (△), 20 (▽).

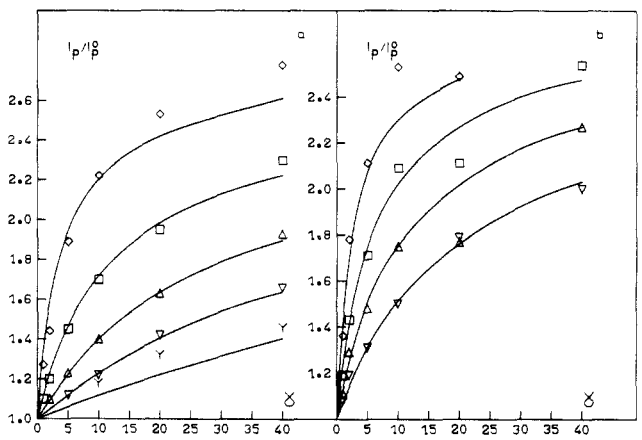

Figure 4. Mediated reduction of *t*-BuCl by biphenyl in DMF + 0.1 M NBu_4BF_4 at 10 °C. Variations of the normalized peak current, i_p/i_p°, with excess factor, $\gamma = C_{RX}^\circ/C_P^\circ$: (a) mediator concentration, C_P° = 1 mM, sweep rate (in $V \cdot s^{-1}$) 0.5 (◇), 2 (□), 5 (△), 10 (▽), 20 (Y); (b) mediator concentration, C_P° = 5 mM, sweep rate (in $V \cdot s^{-1}$) 2 (◇), 5 (□), 10 (△), 20 (▽).

E plots for *n*-BuI and *t*-BuI exhibit a definite downward curvature. This shows that the kinetics of the electrode electron transfer deviates from the Butler–Volmer behaviors, i.e., that the transfer coefficient varies with potential as previously observed for nondissociative electron transfer to organic molecules.[8]

The cyclic voltammetry of the butyl halides on a gold electrode, although not investigated so extensively, showed essentially the same features as on glassy carbon. It was noticed that the reduction peaks are shifted systematically by 50–100 mV in the negative direction.

Mediated Electrochemical Reduction of Butyl Halides. The experiments were carried out as follows. A mediator giving rise to a reversible cyclic voltammogram is selected as a function of the value of its standard potential E_{PQ}°. In a solution of the mediator (concentration: C_P°), increasingly large amounts of the substrate (concentration: C_{RX}°) are added in order to vary the excess factor, $\gamma = C_{RX}^\circ/C_P^\circ$. The normalized peak current i_p/i_p° (i_p, value in the presence of the alkyl halide; i_p°, value in the absence of the alkyl halide) is then plotted as a function of the excess factor, γ. Figures 3 and 4 show two typical examples of such plots obtained with the two systems *t*-BuBr/methyl benzoate and *t*-BuCl/diphenyl for several values of the sweep rate, v, and two values of the mediator concentration, C_P°. The theoretical working curves describing these plots in the context of the catalysis–addition mechanism involving (0)–(3) depend upon two parameters[18b]:

$$\lambda_1 = (k_1/v)(RT/F) \qquad \rho = k_2/(k_2 + k_3)$$

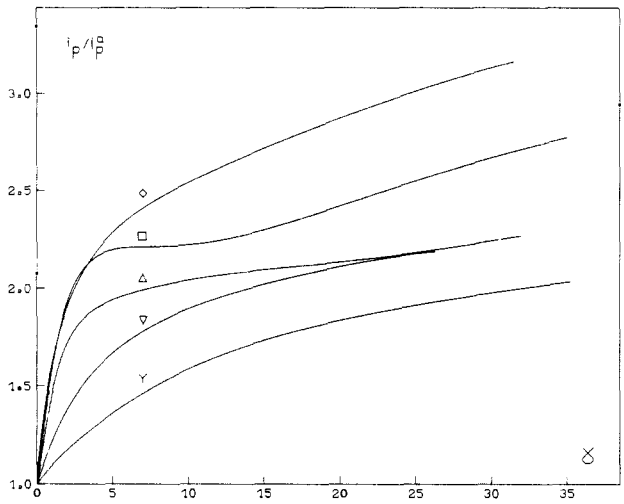

Figure 5. Mediated reduction of *n*-BuI by anthracene in DMF + 0.1 M NBu_4BF_4 at 20 °C. Variations of the normalized current i_p/i_p° with the excess factor $\gamma = C_{RX}^\circ/C_P^\circ$ showing how an increase in sweep rate eliminates the interference of (2′) in the reaction process. Mediator concentration, C_P° = 1 mM, sweep rate (in $V \cdot s^{-1}$) 0.2 (◇), 1 (□), 10 (△), 50 (▽), 200 (Y).

λ_1 is a kinetic parameter measuring the rate of (1) as compared to that of the diffusion process (which is an increasing functon of the sweep rate v). ρ is a parameter which measures the competition between the second electron-transfer step (2) and the addition reaction (3). ρ varies between 0 (prevailing addition) and 1 (prevailing catalysis). In order to carry out a reliable analysis of the kinetic data, one must also take the possible occurrence of (2′) into account. The smaller the sweep rate and the larger the excess factor, the smaller the distance from the electrode surface R· is formed and therefore the larger the contribution of (2′) to the overall catalysis–addition process.[18] It is therefore possible to eliminate the interference of (2′) by raising the sweep rate. Figure 5 illustrates the procedure used to obtain this result. It is seen that at 0.2 $V \cdot s^{-1}$, a plateau is reached around γ = 10. As γ increases further, the i_p/i_p° curve tends to deviate upward from the plateau, featuring the interference of (2′). Increasing the sweep rate delays this deviation up to larger and larger values of γ. In the present case, interference of (2′) can be eliminated up to γ = 30 for sweep rates above 10 $V \cdot s^{-1}$. The data shown in Figures 3 and 4 as well as those concerning all the other mediator–alkyl halides couples we investigated were obtained along the same procedure.

On the other hand, it was considered that as indicated by the above proton donor addition experiments in direct electrochemistry, R^- is protonated by residual water rather than reacting with the starting halide. The possible bimolecular combination of R· leading to dimerization or H-atom disproportionation was neglected in the case of the homogeneous reduction. This stems from the following reasons. When ρ differs from zero, i.e., when the electron-transfer reaction (2) interferes significantly, simulation of the i_p/i_p° vs. γ plot shows the appearance of a maximum as γ increases. This is due to the bimolecular character of the dimerization disproportionation. No such maximum was found experimentally. On the other hand, stoichiometries below two electrons per molecule of mediator were never found. This clearly indicates that when (3) prevails over (2), the bimolecular combination of the R· radicals is also unimportant. We could thus conclude that the latter reaction is negligible in all cases unlike what happens in direct electrochemistry with *t*- and *sec*-BuI. This is actually not very surprizing in view of the fact that the addition reaction (3) has no counterpart in the direct electrochemical process unlike (2) and (2′).

In this context, the data were then treated along a two-parameter (λ_1 and ρ) fitting of the experimental i_p/i_p° vs. data by working curves corresponding to the catalysis addition reaction scheme (eq 0–3). This fitting procedure and the numerical calculation techniques used for obtaining the appropriate working

Table II. Treatment of the Data Shown in Figures 3 and 4

mediator	RX	mediator concn, mM	sweep rate, $V \cdot s^{-1}$	log k_1, $M \cdot s^{-1}$	ρ	k_2/k_3
methyl benzoate	*t*-BuBr	1	2, 5, 10, 20	7.13×10^4	0	0
		4	2, 5, 10, 20	9.12×10^4	0	0
				8.13×10^4 av	0	0
diphenyl	*t*-BuCl	1	0.5, 2, 5, 10, 20	3.83	0.3	0.43
		5	2, 5, 10, 20	3.88	0.3	0.43
				3.85 av	0.3	0.43

curves are described in detail elsewhere.[18b] This treatment was repeated, for each mediator–alkyl halide couple, for several values of the sweep rate and mediator concentration in order to make sure that the assumed reaction scheme (eq 0–3) is correct based on a ±5% error on the determination of i_p/i_p°. The values of log k_1 and ρ were found to be satisfactorily constant upon variation of the sweep rate and mediator concentration. The results of the treatment of the data shown in Figures 3 and 4 are summarized in Table II. The accuracy on the k_1 determination is about ±25%. The same procedure was applied for all the mediator–alkyl halide couples investigated. The corresponding results are reported under the form of supplementary material.

The k_1 and k_2/k_3 average values ultimately obtained are listed in Table III, while the variations of k_1 with the standard potential of the mediator couple E°_{PQ} are represented on Figure 6 for each of the nine butyl halides. As expected, k_1 increases as the potential separation between the reduction of the mediator and that of the alkyl halides diminishes. This is the reason why, for a given butyl isomer, the E°_{PQ} range where data could be obtained becomes more and more positive when passing from Cl to Br and to I. It is noticed that in the overlapping portions of the E°_{PQ} intervals used for each halogen, the values of the competition parameter, k_2/k_3, are the same, within experimental error, for two different halogens which is expected since k_2/k_3 characterizes each R· radical and should therefore be independent of the nature of the halogen. This was indeed observed for the reaction of *m*-toluonitrile, benzonitrile, and methyl benzoate anion radicals with *n*-BuBr and *n*-BuCl and of the *m*-toluonitrile anion radical with *sec*-BuBr and *sec*-BuCl (Table III). This is an important test of the validity of the assumed reaction mechanism, showing, in particular, that the interference of the electrode electron transfer (2′) has been properly eliminated.

Standard Potentials of the RX + e ⇌ R· + X⁻ Reaction. For estimating the values of $E^\circ_{RX/R\cdot + X^-}$ from available thermodynamic data, we used a method similar to that developed by Hush[21a] in the case of methanol as the solvent and further extended by Eberson to other solvents.[21b] Since the E° values in DMF were not available[21b] for all the investigated butyl halides, we recalculate them for the whole series using consistent thermodynamic data. On the other hand, for our purposes, the standard potentials need to be referenced toward the aqueous saturated calomel electrode in DMF.

We first proceed to the estimation of the standard potentials at 25 °C. The standard potential of the RX/R· + X⁻ couple in water vs. the normal hydrogen electrode $E^{\circ,H_2O,NHE}_{RX/R\cdot+X^-}$ is obtained as a combination of the standard free energy of formation of RX, $\Delta G^{\circ,H_2O}_{f,RX}$, R·, $\Delta G^{\circ,H_2O}_{f,R\cdot}$, and X⁻, $\Delta G^{\circ,H_2O}_{f,X^-}$ in water

$$E^{\circ,H_2O,NHE}_{RX/R\cdot+X^-} = \Delta G^{\circ,H_2O}_{f,RX} - \Delta G^{\circ,H_2O}_{f,R\cdot} - \Delta G^{\circ,H_2O}_{f,X^-}$$

(the standard potentials and the free energies are both expressed in volts). It can also be expressed as a function of the standard free energies of formations of RX and R·, $\Delta G^{\circ,g}_{f,RX}$, and $\Delta G^{\circ,g}_{f,R\cdot}$, in the gas phase taking into account the standard free energy ΔG°_4 of the reaction

$$RX^{H_2O} + R\cdot^{g} \rightleftarrows RX^{g} + R\cdot^{H_2O} \qquad (4)$$

$$E^{\circ,H_2O,NHE}_{RX/R\cdot+X^-} = \Delta G^{\circ,g}_{f,RX} - \Delta G^{\circ,g}_{f,R\cdot} - \Delta G^{\circ,H_2O}_{f,X^-} - \Delta G^\circ_4$$

ΔG°_4 is assumed to be approximately the same and equal to the value corresponding to the methyl halides, for all chlorides, bromides, and iodides.[21]

If now the standard potential is referred to the standard Ag^+/Ag electrode in water (unity activity for Ag^+, 0.8 V vs. NHE)

$$E^{\circ,H_2O,Ag^+/Ag}_{RX/R\cdot+X^-} = \Delta G^{\circ,g}_{f,RX} - \Delta G^{\circ,g}_{f,R\cdot} - \Delta G^{\circ,H_2O}_{f,X^-} - \Delta G^\circ_4 - 0.8$$

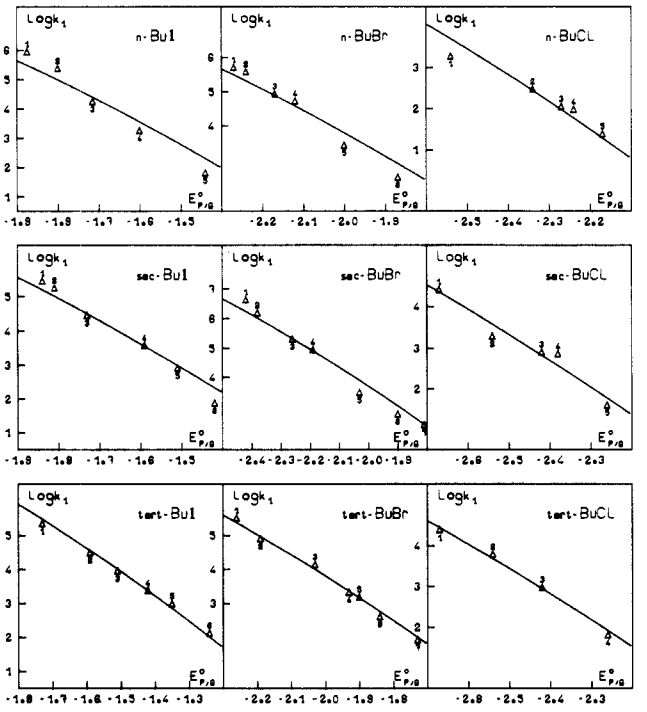

Figure 6. Kinetic characteristics of the reduction of butyl halides by a series of electrogenerated anion radicals in DMF + 0.1 M NBu_4BF_4. Variations of k_1 with E°_{PQ}. The list of mediators corresponding to the numbers close to each point is given in Table IV. The solid line is the best fitting Marcus parabola based on the values of $E^\circ_{RX/R\cdot+X^-}$ given in Table IV. The resulting values of $\Delta G^{\ddagger}_{o,hom}$ are given in Table III.

The value of the standard potential in DMF vs. the standard Ag^+/Ag electrode in DMF is then obtained as

$$E^{\circ,DMF,Ag^+/Ag}_{RX/R\cdot+X^-} = \Delta G^{\circ,g}_{f,RX} - \Delta G^{\circ,g}_{f,X^-} - \Delta G^{\circ,H_2O}_{f,X^-} - \Delta G^\circ_{tr,X^-} - \Delta G^\circ_{tr,Ag^+} - \Delta G^\circ_4 - 0.8$$

where $\Delta G^\circ_{tr,X^-}$ and $\Delta G^\circ_{tr,Ag^+}$ are the standard free energies of transfer from water to DMF of the two ions, assuming that the difference $\Delta G^{\circ,solvent}_{f,RX} - \Delta G^{\circ,solvent}_{f,R\cdot}$ does not vary appreciably when passing from water to DMF.[21] To pass now to the E° value referred toward the aqueous SCE, it suffices to add 0.44 V[26b] to the preceding estimation. Thus, finally,

$$E^{\circ,DMF,aq\,SCE}_{RX/R\cdot+X^-} = \Delta G^{\circ,g}_{f,RX} - \Delta G^{\circ,g}_{f,R\cdot} - \Delta G^{\circ,H_2O}_{f,X^-} - \Delta G^\circ_{tr,X^-} - \Delta G^\circ_{tr,Ag^+} - \Delta G^\circ_4 - 0.36$$

Since $\Delta G^\circ_{tr,Ag^+} = -0.177$ V,[26c]

$$E^{\circ,DMF,aq\,SCE}_{RX/R\cdot+X^-} = \Delta G^{\circ,g}_{f,RX} - \Delta G^{\circ,g}_{f,R\cdot} - \Delta G^{\circ,H_2O}_{f,X^-} - \Delta G^\circ_{tr,X^-} - \Delta G^\circ_4 - 0.183$$

The values of the various free energies used to obtain the standard potential of the RX/R· + X⁻ couple as well as the final

(26) (a) "Handbook of Chemistry and Physics", 52nd ed.; CRC: Cleveland, 1972; p D111. (b) Geske, D. H.; Ragle, M. A.; Bambeneck, J. L.; Balch, A. L. *J. Am. Chem. Soc.* **1964**, *86*, 987. (c) Cox, B. G.; Hedwig, G. R.; Parker, A. J.; Watts, D. W. *Aust. J. Chem.* **1974**, *27*, 477. (d) Stull, D. R.; Westrum, E. F.; Sinke, G. C. "The Chemical Thermodynamics of Organic Compounds"; Wiley: New York, 1969. (e) Benson, S. W. "Thermodynamical Kinetics", 2nd ed.; Wiley: New York, 1976. (f) Wagman, D. D.; Evans, W. H.; Parker, V. B.; Schumm, R. H.; Halow, I.; Bailey, S. M.; Churney, K. L.; Nuttal, R. L. *J. Phys. Chem. Ref. Data* **1982**, *11*, suppl. 2.

Table III. Kinetics of the Homogeneous Reduction of Butyl Halides by Aromatic Anion Radicals

RX	mediator	a	E°_{PQ}, V vs. SCE	log k_1, M^{-1} s^{-1}	ρ	k_2/k_3	av α	$\Delta G^{\ddagger}_{o,hom}$,[d] eV	$\Delta G^{\ddagger,RX/R^{\cdot}+X^-}_{o,iso}$,[e] eV	$\Delta G^{\ddagger}_{o,el}/\Delta G^{\ddagger,RX/R^{\cdot}+X^-}_{o,iso}$	CX stretching wavenumber ν_r,[f] cm^{-1}	$10^6\Delta G^{\ddagger,RX/R^{\cdot}+X^-}_{o,iso}/\nu^2$, eV cm^2
n-BuI[b]	anthracene	1	−1.875	5.95	0.00	0.00						
	9,10-diphenyl-anthracene	2	−1.800	5.38	0.00							
	fluoranthene	3	−1.715	4.26	0.00	0.00	0.56	0.63	1.18	0.73	600	3
	perylene	4	−1.600	3.27	0.00	0.00						
	benzo[*c*]chinoline	5	−1.440	1.82	0.00	0.00						
n-BuBr[b]	*m*-toluonitrile	1	−2.270	5.71	0.55	1.22						
	benzonitrile	2	−2.240	5.59	0.50	1.						
	methyl benzoate	3	−2.170	4.94	0.45	0.82	0.48	0.77	1.38	0.72	640	3.4
	benzo[*h*]chinoline	4	−2.120	4.72	0.20	0.25						
	phenanthridine	5	−2.000	3.44	0.00	0.00						
	anthracene	6	−1.875	2.50	0.00	0.00						
n-BuCl[b]	diphenyl	1	−2.540	3.29	0.95	19.						
	p-toluonitrile	2	−2.340	2.48	0.85	5.67						
	m-toluonitrile	3	−2.270	2.06	0.55	1.22	0.20	0.93	1.70		730	3.2
	benzonitrile	4	−2.240	1.98	0.50	1.						
	methyl benzoate	5	−2.170	1.39	0.45	0.82						
sec-BuI[c]	9,10-diphenyl-anthracene	1	−1.840	5.45	0.00	0.00						
	naphthonitrile	2	−1.810	5.26	0.00	0.00						
	4-cyanopyridine	3	−1.730	4.46	0.00	0.00	0.46	0.74	1.31	0.60	580	3.9
	phthalonitrile	4	−1.590	3.59	0.00	0.00						
	terephthalonitrile	5	−1.510	2.51	0.00	0.00						
	p-diacetylbenzene	6	−1.420	1.89	0.00	0.00						
sec-BuBr[c]	phenanthrene	1	−2.420	6.63	0.50	1.00						
	p-toluonitrile	2	−2.380	6.20	0.43	0.75						
	benzonitrile	3	−2.260	5.32	0.30	0.43	0.40	0.78	1.40	0.64	615	3.7
	methyl benzoate	4	−2.190	4.96	0.15	0.18						
	phenanthridine	5	−2.030	3.48	0.00	0.00						
	anthracene	6	−1.900	2.76	0.00	0.00						
	naphthonitrile	7	−2.010	2.36	0.00	0.00						
sec-BuCl[c]	triphenylphosphine	1	−2.670	4.42	0.80	4.00						
	diphenyl	2	−2.540	3.30	0.70	2.33						
	phenanthrene	3	−2.420	2.91	0.45	0.82	0.35	0.94	1.71		685	3.6
	p-toluonitrile	4	−2.380	2.87	0.33	0.49						
	benzonitrile	5	−2.260	1.60	0.30	0.43						
t-BuI[c]	4-cyanopyridine	1	−1.730	5.35	0.00	0.00						
	phthalonitrile	2	−1.500	4.50	0.00	0.00						
	terephthalonitrile	3	−1.510	3.97	0.00	0.00	0.36	0.68	1.21	0.61	575	3.7
	p-diacetylbenzene	4	−1.420	3.39	0.00	0.00						
	2-nitro-*o*-xylol	5	−1.350	2.99	0.00	0.00						
	3-nitro-*o*-xylol	6	−1.240	2.13	0.00	0.00						
t-BuBr[c]	benzonitrile	1	−2.260	5.50	0.00	0.00						
	methyl benzoate	2	−2.190	4.91	0.00	0.00						
	phenanthridine	3	−2.030	4.15	0.00	0.00	0.37	0.86	1.56	0.60	600	4.3
	9,10-dimethyl-anthracene	4	−1.930	3.34	0.00	0.00						
	anthracene	5	−1.900	3.19	0.00	0.00						
	9,10-diphenyl-anthracene	6	−1.840	2.61	0.00	0.00						
	4-cyanopyridine	7	−1.730	1.93	0.00	0.00						
t-BuCl[c]	triphenylphosphine	1	−2.670	4.39	0.50	1.00						
	diphenyl	2	−2.540	3.79	0.30	0.43						
	phenanthrene	3	−2.420	2.98	0.00	0.00	0.36	0.97	1.79		575	5.4
	benzonitrile	4	−2.260	1.81	0.00	0.00						

[a] Conventional number of the mediator in Figure 6. [b] 20 °C. [c] 10 °C. [d] Homogeneous standard activation free energy from Marcus theory using the E°'s from Table III. [e] Isotopic standard activation free energy (see text). [f] From ref 32.

values of this quantity are summarized in Table IV.

Due to the volatility of the butyl chlorides, particularly *sec*- and *t*-BuCl, the temperature of the experiments was actually selected as lower than 25 °C. In a first series of experiments concerning the homogeneous reduction of the three *n*-butyl halides, the temperature was 20 °C. In a second series involving the homogeneous reduction of the *sec*- and *tert*-butyl halides as well as the direct electrochemistry of all bromides and iodides, the temperature was 10 °C. The temperature effect on the free energy of formation of RX, R·, and X^- in water is very small.[26d] The main sources of variation of the standard potential resides in the variations of the free energies of transfer of Ag^+ and X^- from water to DMF,[26d] the free energy of formation of Ag^+ in water,[26f] and the potential of the standard Ag^+/Ag electrode vs. the aqueous SCE in DMF giving rise to positive shifts of 18, 16, and 6 mV, respectively, from 25 to 10 °C. The standard potentials at 10 °C were thus obtained by adding 40 mV to the 25 °C values. The values at 20 °C were likewise obtained by addition of 10 mV to the 25 °C values. The resulting final values of $E^\circ_{RX/R\cdot+X^-}$ are summarized in the last entry of Table IV.

Discussion

The cyclic voltammetric data described above show that the reduction mechanism depends upon the nature of the halogen and of the butyl moiety. The reductive cleavage of the carbon–halogen bond is easier in the case of iodide than in that of bromide and is easier in the order tert > sec > n. Both the actual reduction potentials (Table I) and the estimated standard potentials (Table

Table IV. Estimation of the Standard Potentials of the RX/R· + X⁻ Couple in DMF vs. Aqueous SCE[a]

compd	$\Delta G^{\circ}_{f,RX}$ [b]	$\Delta G^{\circ}_{f,R\cdot}$ [b]	$\Delta G^{\circ}_{f,X^-}{}^{H_2O}$ [e]	$\Delta G^{\circ}_{tr,X^-}$ [f]	ΔG°_{4} [g]	$E^{\circ,DMF,aq\ SCE}_{RX/R\cdot+X^-}{}_{at}$ 25 °C	temp of expt[j]
n-BuI	0.324[d]	1.554[c]	−0.532	0.194	0.134	−1.209	−1.20[h]
n-BuBr	−0.133[c]	1.554	−1.072	0.311	0.121	−1.230	−1.22[h]
n-BuCl	−0.400[c]	1.554	−1.354	0.475	0.112	−1.369	−1.36[h]
sec-BuI	0.456[d]	1.443[d]	−0.532	0.194	0.134	−0.966	−0.93[i]
sec-BuBr	−0.266[c]	1.443	−1.072	0.311	0.121	−1.252	−1.21[i]
sec-BuCl	−0.551[c]	1.443	−1.354	0.475	0.112	−1.409	−1.37[i]
t-BuI	0.244[c]	1.206[c]	−0.532	0.194	0.134	−0.941	−0.91[i]
t-BuBr	−0.290[c]	1.206	−1.072	0.311	0.121	−1.039	−1.00[i]
t-BuCl	−0.661[c]	1.206	−1.354	0.475	0.112	−1.282	−1.25[i]

[a] All quantities in volts. [b] Standard free energy of formation of RX and R· in the gas phase. [c] From ref 26d. [d] From the incremental method of Benson.[26e] [e] Standard free energy of formation of X⁻ in water, from ref 26f. [f] Standard free energy of transfer of X⁻ from H_2O to DMF from ref 26c. [g] See text, numerical values from ref 21b. [h] 20 °C. [i] 10 °C. [j] See text.

Table V. Analysis of the Electrochemical Reduction Data According to Marcus Theory

compd	D,[a] cm² s⁻¹	Z^{el},[b] cm s⁻¹	$(RT/F)(E_p - E^{\circ})$,[c] at 0.1 V s⁻¹, V	$\Delta G^{\ddagger}_{o,el}$,[d] eV	av value of α at 0.1 V·s⁻¹ theoretl[e]	exptl[f]
n-BuI	1.05×10^{-5}	5.2×10^{3}	47.55	0.80	0.33	0.30
n-BuBr	0.95×10^{-5}	4.6×10^{3}	68.04	0.98	0.30	0.25
sec-BuI	1.05×10^{-5}	5.2×10^{3}	46.31	0.79	0.34	0.33
sec-BuBr	0.95×10^{-5}	4.6×10^{3}	58.20	0.90	0.32	0.25
t-BuI	1.05×10^{-5}	5.2×10^{3}	40.99	0.74	0.35	0.32
t-BuBr	6.95×10^{-5}	4.6×10^{-5}	61.89	0.93	0.31	0.20

[a] Diffusion coefficient estimated according to ref 9 and to the Stokes–Einstein equation. [b] Electrochemical collision frequency calculated from $Z^{el} = RT/2\pi M$, M = molecular weight.[9] [c] E_p = peak potential vs. SCE (Table I). E° from Table III. [d] $\Delta G^{\ddagger}_{o,el}$ estimated from Marcus theory (see text). [e] From Marcus theory. [f] From the peak width (see Table I).

IV) show the same trend. In contrast, the ease of reduction of the alkyl radical is in the order tert < sec < n. Thus, *n*- and *sec*-BuBr and *n*-BuI exhibit a single two-electron reduction wave, leading to R⁻ and then rapidly to RH, the reduction of R· being easier than that of RX. *t*- and *s*-BuI exhibit an opposite behavior. The reduction of RX is easier than that of R·, which leads to the appearance of two successive one-electron waves. At the first wave, the alkyl radicals resulting from the reductive cleavage reaction most probably undergo a bimolecular combination leading to dimerization and/or H-atom disproportionation. At the second wave, they are reduced into R⁻ which then converts into RH. *t*-BuBr seems to fall into an intermediate case where the two processes occur approximately at the same potential.

In both situations, the electrochemical kinetics is controlled by the dissociative electron-transfer reaction

$$RX + 1e \rightleftarrows R\cdot + X^-$$

and thus the cyclic voltammetric data are a source of information on the activation–driving force free-energy relationship characterizing this type of reaction. A first striking observation in this connection is the very low value of the slope of this relationship as measured by the transfer coefficient α (Table I). The question then arises of whether this reflects a situation where α would be low all the way from the standard potential to the reduction potential, i.e., over a potential difference on the order of 1 V, or a situation where α would be potential-dependent starting from α value close to 0.5 at the standard potential and gradually decreasing when going to more negative potentials. The answer to this question is given by the convolution data shown in Figure 2 where it is seen, on the example of *t*- and *n*-BuI, that α does vary with potential. Although not directly observable, a similar dependence should also exist with all the other butyl halides.

On these grounds, we can therefore attempt to treat the cyclic voltammetric data according to a nonlinear activation-driving-force relationship such as the Hush–Marcus relationship[7] based upon a harmonic approximation of the potential energy surface for the reactant and product[27]

$$\Delta G^{\ddagger}_{el} = \Delta G^{\ddagger}_{o,el}\left(1 + \frac{E - E^{\circ}_{RX/R\cdot+X^-}}{4\Delta G^{\ddagger}_{o,el}}\right)^2$$

Table VI. Variation of the Electrochemical Transfer Coefficient with the Potential. Comparison with Marcus Theory

compd	values of α at various potentials (E)[a]	
n-BuI	E	−2.10, −2.40, −2.67
	exptl[b]	0.37, 0.30, 0.22
	theoretl[c]	0.36, 0.31, 0.27
t-BuI	E	−1.60, −1.95, −2.20
	exptl[b]	0.38, 0.35, 0.26
	theoretl[c]	0.38, 0.33, 0.28

[a] In V vs. SCE. [b] From the data shown in Figure 2. [c] From Marcus theory: $\alpha = 0.5 + (E - E^{\circ})/8\Delta G^{\ddagger}_{o,el}$.

($\Delta G^{\ddagger}_{el}$ is the activation free energy of the electrochemical reaction and $\Delta G^{\ddagger}_{o,el}$ its standard value, i.e., its value at the standard potential both expressed in eV). Table V gives the results of such a treatment of the cyclic voltammetric data obtained at 0.1 V·s⁻¹:[28] $\Delta G^{\ddagger}_{o,el}$ is obtained from the peak potential knowing the diffusion coefficient, D, the electrochemical collision frequency, Z^{el},[9] and the standard potential (Table III) according to a numerical

(27) (a) Other nonlinear relationships, such as the Marcus–Agmon–Levine equation for atom transfer[27b,27c] or the Rehm–Weller empirical equation for electron transfer,[27d,e] could also be tried. However, the accuracy of the kinetic data and of the estimation of the standard potentials do not allow a real distinction between these various equations to be made. (b) Marcus, R. A. *J. Phys. Chem.* **1968**, *72*, 891. (c) Agmon, N.; Levine, R. D. *Chem. Phys. Lett.* **1977**, *52*, 197. (d) Rehm, D.; Weller, A. *Ber. Bunsenges. Phys. Chem.* **1969**, *73*, 834. (e) Rehm, D.; Weller, A. *Isr. J. Chem.* **1970**, *8*, 259.

(28) In principle, the rate data should be corrected from the double-layer effects which amounts to replacing the standard potential E° in the Marcus equation by $E^{\circ} + \phi_r$, ϕ_r being the potential difference between the reaction site (usually assumed to be in the outer Helmoltz plane) and the solution.[23b] There is, however, no data available concerning the point of zero charge and the double-layer capacitance, allowing an estimation of ϕ_r for a glassy carbon electrode in DMF with tetrabutylammonium as the supporting electrolyte cation. However, since we observed that the peak potential, for each butyl halide, is about 100 mV more negative on gold than on glassy carbon, since ϕ_r is about the same on gold and on mercury,[28b] and since ϕ_r on mercury is not very different from −100 mV around the reduction potential of the butyl halides,[8d] we do not make a large error when neglecting the double-layer correction in the present analysis. (b) Cápon, A.; Parsons, R. *J. Electroanal. Chem.* **1973**, *46*, 215.

procedure described in ref 22. The transfer coefficient featured by the peak width at 0.1 $V.s^{-1}$ can then be predicted from the $\Delta G^{\ddagger}_{o,el}$ values thus obtained according to the above Marcus equation and compared with the experimental value. There is a good agreement between the two series of values, somewhat better for the iodides than for the bromides.[29]

We now come back to the convolution data obtained with *n*- and *t*-BuI (Figure 2). They can be used to estimate how much the transfer coefficient varies with potential and if this is compatible with the Hush–Marcus equation. This is shown in Table VI where the experimental and theoretical α's taken at three different potentials are compared. It is again seen that the agreement is quite good. It is noticed that the experimental variation is slightly bigger than the theoretical one. This falls in line with the observation that the experimental α's are more distant from the theoretical values with bromides than with iodides, indicating that the variations of the transfer coefficient with potential are somewhat larger than predicted by the Hush–Marcus relationship.

We can thus conclude that the electrochemical kinetics of the reduction of butyl iodides and bromides obey a nonlinear activation–driving force relationship of the Hush–Marcus type corresponding to a concerted electron transfer–bond cleavage reduction of the carbon–halogen bond. This is a further confirmation that under the present experimental conditions, the reduction pathway does not involve the $RX^{-}\cdot$ anion radical as an intermediate. Indeed, if $RX^{-}\cdot$ were an intermediate, the transfer coefficient should be much closer to 0.5 (or even larger than 0.5) since the standard potential of the $RX + e \rightleftarrows RX^{-}\cdot$ reaction is certainly much more negative than that of the $RX + e \rightarrow R\cdot + X^{-}$ reaction, falling in the vicinity of the reduction potential or even negative to it.

In the case of the homogeneous reduction of the butyl halides by electrogenerated aromatic anion radicals, we can consider as discussed earlier that the reaction sequence involves a first-order electron transfer–bond breaking step (eq 1) leading directly to the R· radical. This then undergoes a competitive reduction and coupling with the aromatic radical (eq 2 and 3). For high enough sweep rates, the possible reduction of R· at the electrode surface does not interfere. For a given butyl isomer, the k_2/k_3 ratio decreases as the standard potential of the mediator increases. Accordingly, the magnitude of the k_2/k_3 ratio lies in the order iodide < bromide < chloride. For a given halogen and for the same value of the mediator potential, k_2/k_3 lies in the order *t*-Bu < *sec*-Bu < *n*-Bu. This can be rationalized assuming that the rate constant of the addition reaction is not very sensitive to the nature of the anion radicals, whereas the standard potentials of the $R\cdot/R^{-}$ couples and therefore the rate constant of the reduction of R· by the anion radicals lie in the order *t*-Bu < *sec*-Bu < *n*-Bu. We are currently attempting to determine k_2 and k_3 separately by using the interference of (2′) at low sweep rates.[18c] This should provide a more precise answer to the problem.

Turning back to the kinetics of the initial electron-transfer reaction which is our main purpose in the present paper, the data reported in Figure 6 and Table III show that k_1 is, as expected, a decreasing function of the standard potential of the mediator couple. The analysis of the electrochemical data for the corresponding electron-transfer reaction indicates that the slope of the activation–free-energy relationship varies with potential. A similar behavior should thus be observed in the homogeneous case. The accuracy of the homogeneous rate data does not permit to detect a definite nonlinearity of the log $k_1 - E^{\circ}_{PQ}$ plots (Figure 6). We can, however, see if the same Marcus equation as in the electrochemical case fits with the experimental homogeneous data in terms of overall slope and how the ensuing values of the homogeneous standard free energy of activation $\Delta G^{\ddagger}_{o,hom}$ are related to the corresponding electrochemical quantity $\Delta G^{\ddagger}_{o,el}$. A first observation in this connection is that the slope of the activation–driving force relationship for the homogeneous reaction is larger than in the electrochemical case, the transfer coefficient falling in the range 0.35–0.5 instead of 0.25–0.35 in the electrochemical case. This is simply due to the fact that the potential range of the mediator couples is more positive and thus closer to the $E^{\circ}_{RX/R\cdot+X^{-}}$ than the range of electrode potentials where the reduction wave occurs. The fact that the homogeneous and heterogeneous reactions do obey to the same activation–driving force relationship results from the good fit between the experimental homogeneous data and the Marcus equation as shown in Figure 6. The resulting values of $\Delta G^{\ddagger}_{o,hom}$ are listed in Table III.

$\Delta G^{\ddagger}_{o,hom}$ is related to the isotopic standard activation free energies of the $RX/R\cdot + X^{-}$ and P/Q couples according to

$$\Delta G^{\ddagger}_{o,hom} = \frac{\Delta G^{\ddagger,RX/R\cdot+X^{-}}_{o,iso} + \Delta G^{\ddagger,P/Q}_{o,iso}}{2}$$

The latter quantity is small and approximately constant in the series of aromatic redox couples that were used as mediators. Taking 0.159 eV as an average value,[2a,9] the values of the isotopic standard activation free energies for the $RX/R\cdot + X^{-}$ ensue (Table III).

We can now compare the latter activation free energy to the corresponding electrochemical quantity for all the butyl iodides and bromides. It is seen (Table III) that this ratio is about constant ranging from 0.6 to 0.75,[30] i.e., halfway between what is predicted by Marcus (0.5) and Hush (1) theories, respectively.[7] The first takes into account image force effects in the electrochemical reduction assuming that the distance between the reaction site and the electrode is equal to the radius of a hard sphere equivalent to the molecule, while the second neglects possible image force effects. As discussed earlier, the actual situation may be somewhere in between since the reaction site cannot be much closer to the electrode surface than the outer Helmoltz plane whose distance from the electrode is close to the radius of the bulky tetrabutylammonium cation. Small variations in distance could occur according to the shape of the reactant molecule. In this context, the slight increase of the $\Delta G^{\ddagger}_{o,el}/\Delta G^{\ddagger}_{o,iso}$ observed when passing from *tert*- to *n*-butyl would indicate that the reaction site is closer to the electrode surface in the former case than in the latter. In any case, it is seen that beyond these subtle and difficult to ascertain factors, we can conclude that the homogeneous and heterogeneous processes are governed by essentially the same activation–driving force free energy relationship.

Regarding the structure reactivity relationships, perusal of Tables III–V indicates that the differences between the various butyl isomers are small in terms of both standard potentials and standard activation free energies. In contrast, the differences between the chlorides, bromides, and iodides are quite significant. The E°'s shift negatively when passing from iodides to bromides and to chlorides. As can be seen in Table III, this is mainly due to the fact that the bond energy increases in the same order. The stability of the halogen ions also increases in the same direction but this is not sufficient to compensate the other effect. It is noticed that the standard free energies of activation (Table III) also increase when going from iodides to bromides and chlorides. It follows that at the level of the reduction potentials, the kinetics amplifies the thermodynamics. This is not an unprecedented situation. The same was found with cobalt macrocyclic complexes in the vitamin B_{12} series: the stronger the axial ligand, the more negative the standard potential and the slower the electron transfer.[31] In the framework of an harmonic oscillator model of the reductive cleavage of the carbon–halogen bond, the standard free energy of activation should be related to the stretching fre-

(29) The poorest agreement between the theoretical and experimental value is obtained in the case of *t*-BuBr. In fact, as already noted, the peak is in this case widened by the overlap of the $RX + e \rightarrow R\cdot + X^{-}$ and $R\cdot + e \rightarrow R^{-}$ reduction waves.

(30) Some uncertainty could arise from the fact that the electrochemical data was not corrected for the double-layer effect.[28] However, if we suppose for example that ϕ_r is −100 mV instead of 0, this would result only in a ca. 30-mV error on the $\Delta G^{\ddagger}_{o,el}$'s which have all values above 600 mV (Table IV).

(31) (a) Faure, D.; Lexa, D.; Savéant, J. M. *J. Electroanal. Chem.* **1982**, *140*, 285. (b) *J. Electroanal. Chem.* **1982**, *140*, 295. (c) Lexa, D.; Savéant, J. M. *Acc. Chem. Res.* **1983**, *16*, 235.

quency of the carbon-halogen bond, ν, according to

$$\Delta G^{\ddagger}_{0,iso} = Cst\ \nu^2\ (\Delta d^{\ddagger})^2$$

where $\Delta d^{\ddagger}$ is the difference in the carbon-halogen distance between the initial and the transition states. It is seen that the ratio of $\Delta G^{\ddagger}_{0,iso}$ over ν^2 (Table III) is about constant in all series of butyl halides. The ease of stretching of the carbon-halogen bond thus appears as the dominant factor governing the rate of the reductive cleavage. (The relative variation of location of the transition state vis-à-vis the initial state is less than 20% in the series.)

Concluding Remarks

The main conclusions that emerge from the preceding results and discussion are the following. The kinetics of the heterogeneous and homogeneous reductive cleavage of the carbon-halogen bond in simple aliphatic halides are governed by the same activation-driving force free-energy relationship. It is consistent with a concerted electron transfer-bond breaking mechanism implying that the origin of the driving force scale is the standard potential of the $RX/R\cdot + X^-$ couple and not that of the $RX/RX^{-}\cdot$ couple. The activation-driving force relationship is nonlinear. It can be approximated by a quadratic equation of the Hush-Marcus type. Not unexpectedly, some deviation vis-à-vis this behavior appears for very large values of the driving force.

Experimental Section

Chemicals. The DMF was from commercial origin (Merck) and was vacuum-distilled before use. The supporting electrolyte (Fluka puriss.) was used as received. The butyl halides, from commercial origin, were distilled before use, and the mediators were used as received.

Instrumentation. The electrochemical cell was equipped with a water jacket, allowing the temperature to be fixed by means of a thermostat (10 °C with the *t*- and *sec*-Bu halides and 20 °C with the *n*-butyl halides). For direct electrochemical experiments, the working electrode was in all cases a glassy carbon (IMC Industry, Japan—Grade CG-A) disc of 3-mm diameter. This was polished by using a 1-μm diamond paste and ultrasonically rinsed in ethanol before use. Several control experiments were carried out with a gold disc electrode (1-mm diameter) pretreated in the same way. A mercury drop suspended from a 1-mm gold disc was used as the working electrode for the mediated electrochemical reduction experiments. It was checked with several mediator-alkyl halide couples that the results are the same as with a glassy carbon electrode. The counterelectrode was a mercury pool and the reference electrode an aqueous SCE in all cases.

The cyclic voltammetry apparatus was composed of a home-built solid-state amplifier potentiostat equipped with positive feedback *iR* drop compensation and a PAR (Model 175) function generator. The voltammograms were displayed on a chart recorder (Ifelec 2502) for sweep rates below 0.5 $V.s^{-1}$. For higher sweep rates, a Nicolet (3091) allowing the automatic determination of peak heights and peak potential was used.

The numerical calculations were carried out on a MINI 6 BULL computer and all the figures (with the exception of Figures 1 and 2) were directly drawn on a 1102 Benson plotter.

Acknowledgment. The attribution of a fellowship to I. G. by the Ministerio de Educación y Ciencia is gratefully acknowledged. Discussions with Prof. L. Nadjo (Université de Nancy, France) during the initial stage of this work were very fruitful.

Registry No. *n*-BuI, 542-69-8; *n*-BuBr, 109-65-9; *sec*-BuI, 513-48-4; *t*-BuI, 558-17-8; *sec*-BuBr, 78-76-2; *t*-BuBr, 507-19-7; *n*-BuCl, 109-69-3; *sec*-BuCl, 78-86-4; *t*-BuCl, 507-20-0.

Supplementary Material Available: Kinetic data for the reduction of butyl halides, i_p/i_p° vs. γ plots of mediators, and λ_1 and ρ parameter fittings of each butyl halide (76 pages). Ordering information given on any current masthead page.

(32) (a) Rao, C. N. R. "Chemical Applications of Infrared Spectroscopy"; Academic Press: New York, 1963; pp 308-309. (b) "Handbook of Chemistry and Physics", 52nd ed.; CRC: Cleveland, 1972; pp F202, F.203.

Semiconductor Photocatalysis.[1] Cis-Trans Photoisomerization of Simple Alkenes Induced by Trapped Holes at Surface States

Shozo Yanagida,* Kunihiko Mizumoto, and Chyongjin Pac

Contribution from Chemical Process Engineering, Faculty of Engineering, Osaka University, Suita, Osaka 565, Japan. *Received May 13, 1985*

Abstract: The use of ZnS or CdS as photocatalysts induces an efficient cis-trans photoisomerization of simple alkenes, e.g., the 2-octenes, 3-hexen-1-ols, and methyl 9-octadecenoates in photostationary cis-trans ratios almost identical with the thermodynamic equilibrium ratios achieved by the phenylthio radical. Quantum yields for the cis-trans photoisomerization, ϕ_{c-t}, exceed largely over unity. Mechanistic studies involving Stern-Volmer analyses, quenching effect of oxygen, and ESR analyses under band-gap irradiation of ZnS in methanol demonstrate that the photoisomerizations take place with high turnover numbers at active sites where trapped holes at surface states, i.e., sulfur radicals arising from Zn vacancies and/or interstitial sulfur on sulfide semiconductors, play decisive roles. A highly efficient catalysis occurs with ZnS sols prepared from polysulfide-containing Na_2S solution. The trapped-hole mechanism is further supported by the enhanced effect of water acting as a good electron acceptor as well as the quenching effect of diethylamine acting as an electron donor.

Photoreactions at semiconductor/liquid or vapor interface are generally discussed based on the separation of electrons and holes upon absorption of photons.[2] The separated electron and hole are considered to migrate to the surface of the irradiated semiconductor on which photoredox reactions occur. Our recent studies revealed that not only the reductive H_2 generation but also sequential two-electron reductions of organic substrates occur efficiently on ZnS without noble metal modification and that the one-hole oxidation which leads to carbon-carbon bond formation or the two-hole oxidation through intermediary carbocation is observable depending on organic substrates and reaction conditions.[3] On the other hand, photoinduced organic reactions without

(1) Part 6. Part 5: Yanagida, S.; Kizumoto, H.; Ishimaru, Y.; Pac, C.; Sakurai, H. *Chem. Lett.* **1985**, 141.

(2) (a) Bard, A. J. *J. Photochem.* **1979**, *10*, 59. (b) Grätzel, M. "Energy Resources through Photochemistry and Catalysis"; Academic Press: New York, 1983.

(3) (a) Yanagida, S.; Azuma, T.; Sakurai, H. *Chem. Lett.* **1982**, 1069. (b) Yanagida, S.; Azuma, T.; Kawakami, H.; Kizumoto, H.; Sakurai, H. *J. Chem. Soc., Chem. Commun.* **1984**, 21. (c) Yanagida, S.; Kawakami, H.; Hashimoto, K.; Sakata, T.; Pac, C.; Sakurai, H. *Chem. Lett.* **1984**, 1449. (d) Yanagida, S.; Azuma, T.; Midori, Y.; Pac, C.; Sakurai, H. *J. Chem. Soc., Perkin Trans. 2* **1985**, 1487. (e) Yanagida, S.; Kizumoto, H.; Ishimaru, Y.; Pac, C.; Sakurai, H. *Chem. Lett.* **1985**, *141*.

0002-7863/86/1508-0647$01.50/0